Preparation and Characterization of Ultrafine Co and Ni Particles in a Polymer Matrix

A. Sarkar,[†] S. Kapoor,*[,†] G. Yashwant,[‡] H. G. Salunke,[‡] and T. Mukherjee[†]

Radiation Chemistry & Chemical Dynamics Division and Technical Physics and Prototype Engineering Division, Bhabha Atomic Research Centre, Trombay, Mumbai 400 085, India

Received: December 2, 2004; In Final Form: February 3, 2005

A facile route for in situ synthesis of Co and Ni nanoparticles in a preorganized polyacrylamide gel is reported. Metal−polymer composites were prepared by γ-irradiation at room temperature. The Co nanoparticles were roughly 3−5 nm in size and were stable in the polymer matrix in the presence of air. The presence of Co and Ni nanoparticles was established by their ability to transfer an electron to methyl viologen {paraquat: 1,1′-dimethyl 4,4′-dipyridinium dichloride; MV^{2+} $(Cl^-)_2$}. The Co and Ni nanoparticles were probed for their magnetic characteristics by a superconducting quantum interferometer device (SQUID) magnetometer and display a low superparamagnetic blocking temperature T_B of about 13 and 10 K, respectively. The field-dependent magnetic behavior below T_B displays the standard features corresponding to superparamagnetism, as expected for very small Co and Ni crystallites. This also suggests that particles are polycrystalline in nature.

Introduction

Due to quantum size effect the synthesis of metal and semiconductor nanoparticles has been the subject of research in a wide range of fields.[1−6] Metallic nanoparticles such as silver, copper, and gold have been studied because their surface plasmon absorption band appears in the visible range and hence it becomes easy to monitor the changes in their physicochemical properties with variation in size or due to adsorption of molecules on their surface.[6] Metal nanoparticles are of great interest in terms of their potential applications in various fields such as biomedical, electronic, and optical devices. Recently, nanocomposites of inorganic/organic materials have become important for their role in numerous applications.[1] Incorporation of metal nanoparticles in polymer matrixes has been gaining particular importance due to the possible applications in material engineering.[2] Conventionally, the composites are made by mechanically mixing the metal nanoparticles into molten or dissolved polymer matrixes.[7−11] This often leads to an inhomogeneous dispersion of particles. Very recently, considerable attention has been paid to the in situ synthesis of metal nanoparticles in polymer matrixes.[12−18] In such syntheses, dissolution of the metal salt was done in the monomer followed by polymerization and reduction of metal ions, using UV/γ-radiation and thermal processes.

Magnetic nanoparticles have been, and continue to be, of great interest due to their expected application, e.g., in high-density magnetic recording or magnetic sensor.[19−22] Nanoparticles less than about 14 nm for Co are magnetically single domains in character. For particles smaller than 5 nm, for Co, the magnetic anisotropy energy per particle becomes comparable to the thermal energy (kT). Due to this thermal fluctuation induce random instabilities on the magnetic moment with time and the particle becomes superparamagnetic.[24] To make material of high magnetization it is important to prepare noncontaminated surfaces, as magnetization is highly sensitive to surface contamination. Recently Alivisatos[25] et al. have demonstrated that by using a mixture of oleic acid and TOPO, magnetic nanorods of Co can be prepared. However, the rods are not stable in the reaction medium and transform into spheres with time. Similarly, only a few cases of the preparation of Ni nanoparticles, by chemical reduction and by using an oil bath or microwave heating in aqueous solution and organic media,[26−30] have been reported.

For many applications, the nanoparticles have to be inside a dielectric matrix. These metal−dielectric composites prepared below the percolating limit should exhibit nonlinearity in their optical and electronic properties.[31] In addition, incorporation of particles in polymer matrix may make them resistant to aerial oxidation. Though numerous studies on noble metal nanoparticles in polymers have been reported in the literature,[15−17] very little is known about the possible uses of other transistion metal nanoparticles.[18] Among numerous methods for the preparation of metal/polymer composites, radiolytic and photolytic methods are very popular because of the ease in the preparation of nanoclusters of narrow size distribution. In the present work, we report for the first time that the radiolytic approach can be used for the in situ formation of fine Co and Ni metal nanoparticles entrapped in preorganized polyacrylamide matrix.

Experimental Section

Materials. Acrylamide (BDH), $CoSO_4$ (BDH), $NiSO_4$ (BDH), propan-2-ol (Spectrochem, India), and methyl viologen dichloride (Aldrich) were used as received. Water purified by a Millipore system was used for making the solutions.

Preparation of Polymer Matrix and Colloidal Metal Particles. Metal salt (1×10^{-2} mol dm^{-3}), propan-2-ol (5 mol dm^{-3}),and organic monomer acrylamide (3.52 mol dm^{-3}) were mixed in water. The solution was deaerated by bubbling with N_2 (>99.9%) before γ-irradiation at normal pressure and at room temperature. The total dose used for irradiation was 35 kGy at a dose rate of 0.9 kGy h^{-1}.

* Address correspondence to this author. Fax: (+)- 91-22-25505151. Phone: (+)-91-22-25590298. Email: sudhirk@apsara.barc.ernet.in.
[†] Radiation Chemistry & Chemical Dynamics Division.
[‡] Technical Physics and Prototype Engineering Division.

10.1021/jp044521a CCC: $30.25
Published on Web 03/22/2005

Characterization. The resulting composite materials were characterized at room temperature by UV−visible absorbance (Spectroscan UV 2600 Chemito spectrophotometer), transmission electron microscopy (TEM) (JEOL JEM-2000FX electron microscope), energy-dispersive X-ray spectrometry (XRF), and superconducting quantum interferometer device (SQUID) magnetometer measurements. The energy-dispersive X-ray spectrometry employed in the present work (XRF) consists of SLP series EG & G ORTEC and Si(Li) detector of 28 $mm^2 \times 5$ mm size. It has an energy resolution of 170 eV at 5.9 keV Mn K−X-rays. The annular geometry of a $^{241}Am_{95}$ radioisotope source having photon flux at around 10^8photons/s was used for excitation at characteristic X-ray. A PC based 8 K MCA with PCA 95 software was used for data analysis.

Results and Discussion

Preparation of Co/Ni Nanoparticles−Polymer Composites. The primary radicals of water radiolysis (reaction 1) produced on γ-irradiation are[32]

$$H_2O \rightsquigarrow e_{aq}^-, H^\bullet, {}^\bullet OH \qquad (1)$$

Taking into consideration the rate constants of acrylamide toward $^\bullet$H and $^\bullet$OH radicals[33] it can be calculated that at the concentrations used in the present system all the $^\bullet$H atoms are scavenged by acrylamide. However, only 70% of the $^\bullet$OH radicals get scavenged by acrylamide and the remaining 30% by 2-propanol. Since the concentration of the monomer used is high, initially the polymerization of acrylamide monomer occurs via primary and secondary radicals. It is important to point out here that during irradiation first a gel like material was formed. This is not surprising, as polyacrylamide is a crystalline as well as membrane forming hydrophilic polymer, therefore, it can undergo gelation reaction (physical and chemical) due to cross-linking of the polymer. This was followed by the change in color of the gel due to the reduction of the metal ion. Finally, the gel matrix became uniformly brown in color and no sign of segregated Co and Ni particles was observed in the matrix. This could be due to the binding of initial metal clusters in the gel (polymer chains) that inhibits the aggregation of Co or Ni particles. Stabilization of metal nanoparticles in the polymer can also be explained on the basis of increase in the viscosity of the solution.

The resulting composite materials of Co and Ni nanoparticles, formed after irradiation, were characterized by their absorption spectra and showed similar features as are reported in the literature.[34,35] A representative case is shown in Figure 1. It can be seen that the absorbance due to Co nanoparticles was so intense (Figure 1a) that it was not possible to measure its absorption at lower wavelengths. To check the stability of the particles in air, the gel was spread over a Petri dish and was exposed to air. It was observed that the prepared Ni metal/organic nanocomposites were stable in air for 1 day without any noticeable change in the color as well as optical absorption. After this period, slow fading of the color, that is, oxidation of metal nanoparticles started. However, in the case of Co metal/organic nanocomposites it was observed that the gel containing Co metal particles on exposure to air became hardened and the particles were stable for around 2 months. After this, the color of the hardened gel started changing, that is, it acquired the color of Co^{2+} ions. It is important to mention here that Co and Ni particles in aqueous solution are highly reactive and are oxidized instantaneously on exposure to air.[34,35] This experiment clearly shows that the stability of the Co metal particle increased

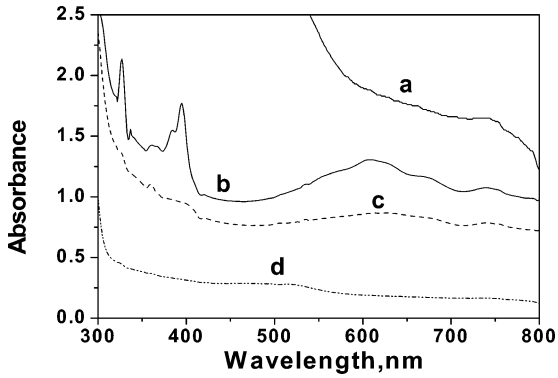

Figure 1. (a) UV−vis absorption spectrum of Co nanoparticles−polymer composites prepared by γ-irradiation (dose = 79.2 kGy) of N_2-bubbled aqueous solutions containing acrylamide (3.52 mol dm^{-3}), propan-2-ol (5 mol dm^{-3}), and $CoSO_4$ (1×10^{-2} mol dm^{-3}). (b) UV−vis absorption spectrum of the $MV^{+\bullet}$ radical 5 days after adding MV^{2+} ($\sim 1 \times 10^{-3}$ mol dm^{-3}) to the solution obtained in part a and (c) after exposing the solution obtained in part b to air. (d) Absorption spectrum of Co^{2+} ions in the matrix before irradiation.

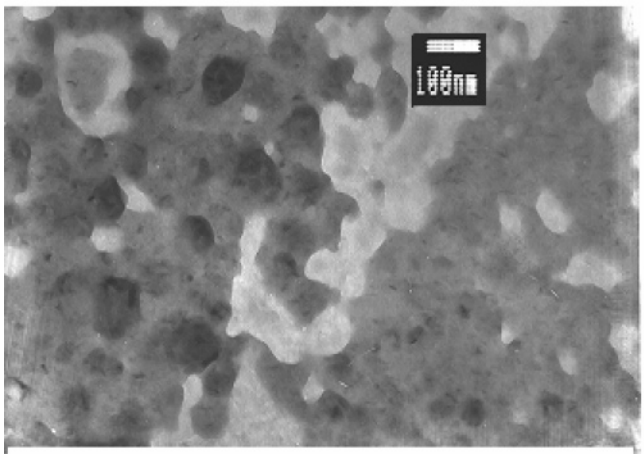

Figure 2. TEM image of Co metal nanoparticles. Other conditions are the same as in Figure 1a.

enormously in the polymer. This is due to the fact that the rate of permeation of oxygen into the polymer is slow. As mentioned earlier, the matrix was gellike and therefore attempts to characterize the particles by XRD failed due to the broadening of the peaks. However, the presence of Co and Ni in the polymer matrix was ascertained by the technique of energy-dispersive X-ray fluorescence and TEM. The TEM images of the Co nanoparticles thus produced are displayed in Figure 2. It is clear from TEM images that the Co nanoparticles prepared by the above procedure are somewhat polydisperse in nature with an average size of 3−5 nm.

Electron-Transfer Reactions. It is known that metal nanoparticles are highly reactive[6,34,35] and transfer electrons to O_2 and MV^{2+}. Transfer of electrons from metal nanoparticles to MV^{2+} can be monitored with a spectrophotometric technique. The $MV^{+\bullet}$ radical formed after electron transfer is blue and has a strong absorption in the visible region.[36] In the case of O_2, fading of the color of the matrix takes place after electron transfer. As mentioned above that metal particles were trapped in the gel network, it is interesting to see whether the metal particles incorporated in a polymer matrix can still transfer electrons to MV^{2+}. To check this, a deaerated aqueous solution of MV^{2+} (10^{-2} mol dm^{-3}) was injected above the metal−polymer composite layer. It was noticed that the polymer matrix developed a blue color slowly. Initially, only the top layer

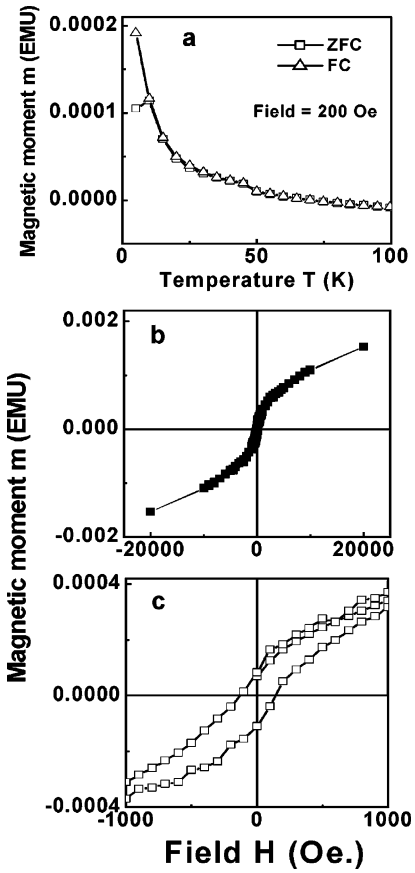

Figure 3. (a) FC and ZFC magnetization vs temperature curves with $T_B = 10$ K for the sample Ni nanoparticles obtained in polyacrylamide gel on irradiation (dose = 86.4 kGy) of N_2-bubbled aqueous solutions containing acrylamide (3.52 mol dm^{-3}), propan-2-ol (5 mol dm^{-3}), and $NiSO_4$ (1×10^{-2} mol dm^{-3}). The curves were recorded at 200 Oe. (b) Magnetization vs applied field hysteresis loop at 5 K for the sample (Ni) observed in part a. (c) Enlargement of part b at low field.

became blue; however, after 5 days the whole gel matrix became bluish and the corresponding spectrum is shown in Figure 1b. On exposure to air, the gel matrix became colorless over a period of time (Figure 1c). For comparison, the absorption spectrum of Co^{2+} ions in the matrix is also shown in Figure 1d. It is known that the reduction of MV^{2+} into $MV^{+\bullet}$ radical by electron transfer from metal particles shows that metal particles are of nanometer size.[6] This further established that the prepared Co and Ni particles were of nanometer size.

Magnetization Studies of the Nanocomposites. Magnetic response of the composite materials was measured with a SQUID magnetometer. Figures 3 and 4 show the magnetic susceptibilities for Ni and Co nanoparticles, respectively. As can be clearly seen, the curves of temperature-dependent zero field cooled (ZFC) and field cooled (FC) susceptibilities are typical of magnetic materials. The magnetic properties of Co and Ni nanoparticles were also investigated as a function of external field (Figures 3 and 4). The presence of magnetic transition temperature (T_B) was measured by estimating the deviation in ZFC and FC measurements. The field cooling mode consists of applying the field far above the transition temperature and then cooling the sample in the applied field to $T < T_B$. Zero field cooling consists of first cooling the sample in zero field to $T < T_B$ and then applying a nonzero field. Magnetic data are obtained by raising the temperature to $T \gg T_B$, keeping the magnetic field constant. In the present measurements on Co and Ni, a field of 200 Oe was applied for ZFC/FC measurements. Considering the size of particles ($\approx$ 3−5 nm) the 200 Oe applied field can be considered reasonably small.

Magnetization of the material for a given applied field (H) and at a given temperature is ensemble averaged over all possible magnetization states in the system and is given by

$$M(H,T) = \frac{\sum_{\text{states}(i)} M_i(H) e^{-E(H)/k_B T}}{\sum_n e^{-E(H)/k_B T}} \qquad (2)$$

The magnetic energy contribution to $E(H)$ (viz. $\approx \bar{\mu}_s(\bar{H}_{ext} + \bar{H}_{int})$) is due to the external applied field, $\bar{H}_{ext}$, as well as interaction between the moments and the Curie−Weiss field, $\bar{H}_{int}$. A system of coupled magnetic moments will respond differently when they are cooled in the presence or absence of magnetic field. As seen in eq 2, the difference arises due to competing contribution of thermal energy ($=k_BT$) vis-à-vis magnetic energy terms ($\approx \bar{\mu}_s(\bar{H}_{ext} + \bar{H}_{int})$) to total free energy. Thermal energy k_BT tends to randomize magnetic moment on atoms, while $\langle \approx \bar{\mu}(\bar{H}_{ext} + \bar{H}_{int}) \rangle$ tends to align the moment in the direction of the applied field. Above the transition temperature (viz. T_B), ZFC/FC behavior would be identical due to $k_BT > \bar{\mu}_s\bar{H}_{ext}$ (for small H_{ext}) resulting in paramagnetic behavior. Below T_B, the presence of $\bar{\mu}_s\bar{H}_{int}$ terms bring in deviation of ZFC/FC behavior (see, e.g., Figures 3 and 4). The magnetic transition temperature is the blocking temperature (T_B). Below T_B the magnetization vs T behavior depends on the type of coupling constant. For ferromagnetic coupling, ZFC behavior below T_B is nearly independent of temperature. For antiferromagnetic coupling, the magnetization rapidly goes to zero below T_B. For intermediate coupling (viz. ferrimagnetic or superparamagnetic behavior), the magnetization does not vanish to zero, but saturates to a nonzero value. The ZFC and FC cycles in an external field of 200 Oe demonstrate that samples exhibit magnetic behavior at low temperatures. Also, it is clear that Ni and Co nanoparticles in polymer matrix possess a blocking temperature T_B of about 10 and 13 K, respectively. The narrow cusp in ZFC, Figures 3a and 4 (parts a and b) indicates a narrow size distribution, deduced from the normal energy barrier distribution and the relaxation times of the magnetic moments of the particles. Also important to note is that below T_B, the magnetization does not vanish rapidly to zero (see Figure 4b for Co marked with an arrow). Nonzero magnetization below T_B implies that the material has a ferrimagnetic ordering. It can be noted in Figure 4 (parts a and b) that ZFC becomes saturated at ~5 K for Co, indicating a ferrimagnetic ordering. Since bulk Co is known to have a higher magnetic transition temperature ($\approx$1388 K) and higher magnetic moment per atom (1.72 μ_B), a blocking temperature of 10−13 K for both materials implies that average Co intercluster separation was larger than that of Ni.

Assuming a typical time of measurement for the dc magnetization experiments, the blocking temperature T_B for a particle of volume V and uniaxial anisotropy constant K_0 is given by[36,37]

$$T_B = \frac{K_0 V}{25 k_B} \qquad (3)$$

where k_B is the Boltzmann constant (1.38×10^{-16}). Assuming spherical particles of 3 nm in diameter for Co particles and taking the blocking temperature as 13 K, the effective anisotropy constant is 3.17×10^6 erg cm^{-3}.

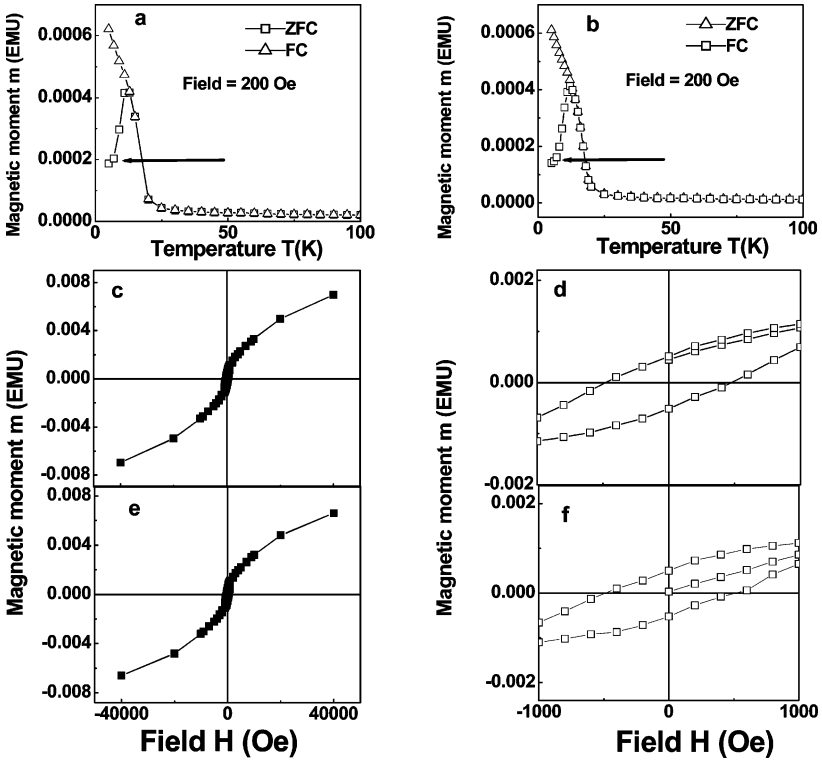

Figure 4. (a) FC and ZFC magnetization vs temperature curves with $T_B = 13$ K for the Co nanoparticle−polymer composite obtained in polyacrylamide gel on irradiation (dose = 86.4 kGy). Other conditions are the same as in Figure 1a. The magnetization was recorded after exposing the sample to air for 1 day. The curves were recorded at 200 Oe. It may be noted that ZFC becomes saturated at ~5 K. (b) FC and ZFC magnetization vs temperature curves with $T_B = 13$ K for the Co nanoparticle−polymer composite prepared similarly as the sample observed in Figure 3a. The magnetization was recorded after exposing the sample to air for nearly two months. The curves were recorded at 200 Oe. It may be noted that ZFC becomes saturated at ~5 K. (c) Magnetization vs applied field hysteresis loop at 5 K for the sample (Co) observed in part a. (d) Enlargement of part c at low field. (e) Magnetization vs applied field hysteresis loop at 5 K for the sample (Co) observed in part b. (f) Enlargement of part e at low field.

TABLE 1: Coercive Force and Remanence Magnetization for Various Metal−Polymer Composites

sample	coercive force (Oe)	remanence (EMU)
Ni	130	8.38×10^{-5}
Co−A	83	2.73×10^{-4}
Co−B	478	5.14×10^{-4}
Co−C	509	5.02×10^{-4}

The hysteresis loops for Ni and Co nanoparticles were measured at 5 K and are shown in Figures 3 and 4. The weak hysteresis and linear variation of magnetization with temperature revealed that Co and Ni nanoparticles were nearly superparamagnetic. This could be attributed to the fact that Co and Ni nanoparticles were so small in size that they can be considered to have single magnetic domains. The existence of an hysteresis loop at 5 K confirms ferrimagnetic (or superparamagnetic) ordering at 5 K. However, hysteresis does not show the presence of saturation (at 4 T) as in bulk Co or Ni. The absence of saturation magnetization can be attributed to well-dispersed clusters in the polymer matrix. Since the clusters are dispersed, the intercluster coupling in the material is weak resulting in the absence of long-range ordering in the material. However, within the cluster, the ordering is complete at 5 K, resulting in hysteresis-like behavior at lower fields.

The remanence and coercive force for Ni and Co are given in the Table 1. As observed in the table for samples of Co-A and Ni, although remanences are similar in magnitude, the coercive force for Ni is more than that for Co. It is pertinent to mention here that the sample size (0.3 mL) as well as the experimental conditions were identical in both the cases. Smaller coercive force in Co could be attributed to a well-dispersed solution (lower concentration) resulting in weak intercluster coupling and a concomitant lower coercive force.

As discussed above the Ni sample underwent oxidation and loss of magnetization after exposure to air, while Co retained the cluster nature up to nearly two months after exposure to air. To further confirm the quality of Co nanocrystallites on exposure to air, magnetic measurements were carried out for samples exposed to air for different durations. In the table are given three categories of Co measurements, viz., Co−A (metal−polymer composite matrix with moisture under inert conditions), Co−B (metal polymer composite after exposure to air for 1 day), and Co−C (metal polymer composite after exposure to air for nearly two months). Magnetization measurements carried out on Co samples after around 2 months of synthesis, Figure 4 (parts b, e, and f), confirm the presence of magnetization in the material. No significant change in the magnetization values as well as in T_B was observed. This shows the absence of agglomeration in Co in a polymer matrix. Figure 4 (parts e and f) shows hysteresis for Co materials after two months of exposure to air. When compared with the sample exposed to air for only 1 day (Figure 4, parts c and d), we conclude that cobalt nanocrystallites have not undergone either agglomeration or oxidation.

Conclusion

An easy method for the synthesis of metal−polymer nanoparticulate systems is reported. This is probably the first report showing the stability of Co-polymer composites at room temperature. The magnetic characteristics of the Co and Ni nanoparticles are in accordance with those expected for nano-

scale superparamagnetic particles. The blocking temperature where the magnetic directions of individual grains essentially remain invariant was determined to be 10 and 13 K for Ni and Co nanoparticles, respectively. The blocking temperature for Co-polymer composite remains almost constant even on exposing the sample to air for 2 months. The present work shows the advantage of stabilizing magnetic metal nanoparticles in a gel matrix.

References and Notes

(1) Fendler, J. H. *Chem. Rev.* **1987**, *87*, 877.
(2) Schmid, G. *Chem. Rev.* **1992**, *92*, 1709.
(3) Kamat, P. V. *Chem. Rev.* **1993,** *93*, 267.
(4) Lewis, L. N. *Chem. Rev.* **1993**, *93*, 2693.
(5) Gates, B. C. **1995**, *95*, 511.
(6) Henglein, A. *Chem. Rev.* **1989**, *89*, 1861.
(7) Dirix, Y.; Bastiaansen, C.; Caseri, W.; Smith, P. *J. Mater. Sci* **1999**, *34*, 3859.
(8) Ottaviani, M. F.; Valluzzi, R.; Balogh, L. *Macromolecules* **2002**, *35*, 5105.
(9) Sarma, T. K.; Chowdhury, D.; Paul, A.; Chatopaddhyay, A. *Chem. Commun.* **2002**, 1048.
(10) Shiraishi, Y.; Toshima, N. *Colloids Surf. A* **2002**, *169*, 59.
(11) Ghosh, K.; Maiti, S. N. *J. Appl. Polym. Sci.* **1996**, *60*, 323.
(12) Hatchett, D. W.; Josonicz, M.; Janata, J.; Baer D. R. *Chem. Mater.* **1999**, *11*, 2989.
(13) Southward, R. E.; Boggs, C. M.; Thompson, D. W.; Clair, A. K. S. *Chem. Mater.* **1998**, *10*, 1408.
(14) Gotoh, Y.; Igarashi, R.; Ohkoshi, Y.; Nagura, M.; Akamatsu, K.; Deki, S. *J. Mater. Chem.* **2002**, *10*, 2548.
(15) Zhu, Y. J.; Qian, Y. T.; Li, X. J.; Zhang, M. W. *Chem. Commun.* **1997**, 1081.
(16) Liu, H. R.; Ge, X. W.; Ni, Y. H.; Ye, Q.; Zhang, Z. C. *Radiat. Phys. Chem.* **2001**, *61*, 89.
(17) Zhang; Z. P.; Zhang, L. D.; Wang, S. X.; Chen, W.; Lei, Y. *Polymer* **2001**, *42*, 8315.
(18) Kapoor, S.; Joshi, R. J.; Mukherjee, T. *J. Colloid Interface Sci.* **2003**, *267*, 74.
(19) Schmid, G. In *Clusters and Colloids, from Theory to Application*; VCH: Weinheim, Germany, 1994.
(20) Hadjipanayis, G. C.; Siegel, R. W. *Nanophase Materials*; Kluwer: Dordrecht, The Netherlands, 1994.
(21) Liu, K.; Nagodawithana, K.; Searson, P. C.; Chien, C. L. *Phys. Rev. B* **1995**, *51*, 7381.
(22) Petit, C.; Taleb, A.; Pileni, M. P. *J. Phys. Chem. B* **1999**, *103*, 1805.
(23) Gould, P. *Mater. Today* **2004**, *February*, 36.
(24) Martin, J. I.; Nogues, J.; Liu, K.; Vicent, J. L.; Schuller, I. K. *J. Magn. Magn. Mater.* **2003**, *256*, 449.
(25) Puntes, V. F.; Krishnan, K. M.; Alivisatos A. P. *Science* **2001**, *291*, 2115.
(26) Cordente, N.; Respaud, M.; Senocq, F.; Casanove, M.-J.; Amiens, C.; Chaudret, B. *Nano Lett.* **2001**, *1*, 565.
(27) Chen, D.-H.; Hsieh, C.-H. *J. Mater. Chem.* **2002**, *12*, 2412.
(28) Hou, Y.; Gao, S. *J. Mater. Chem.* **2003**, *13*, 1510.
(29) Kurihara, L. K.; Chow, G. H.; Schoen, P. E. *Nanostruct. Mater.* **1995**, *5*, 607.
(30) Chen, D. H.; Wu, S. H. *Chem. Mater.* **2000**, *12*, 1354.
(31) Schalaev, V. M. *Phys. Rev. B* **1998**, *57*, 13265.
(32) Spinks, J. W. T.; Wood, R. J. *An introduction to Radiation Chemistry*, 3rd ed.; John Wiley and Sons: New York, 1990; p 243.
(33) Buxton, G. V.; Greenstock, C. L.; Helman, W. P.; Ross, A. B. *J. Phys. Chem. Ref. Data* **1988**, *17*, 513.
(34) (a) Georgopoulos, M.; Delcourt, M.-O. *New J. Chem.* **1989**, *13*, 519. (b) Marignier, J. L.; Belloni, J.; Delcourt, M.-O.; Chevalier, J. P. *Nature* **1985**, *317*, 344.
(35) Ershov, B. G.; Sukhov, N. L.; Janata, E. *J. Phys. Chem. B* **2000**, *104*, 6138.
(36) Ebbesen, T. W.; Levey, G.; Patterson, L. K. *Nature* **1982**, *298*, 545.
(37) Dormann, J. L.; D'Orazio, F.; Lucari, F.; Tronc, E.; Prene, P.; Fiorani, D.; Cherkaoui, R.; Nogues, M. *Phys. Rev. B* **1996**, *53*, 14291.
(38) Chen, Q.; Zhang, Z. L. *Appl. Phys. Lett.* **1998**, *73*, 3156.